

Diagnostic and prediction value of synthetic magnetic resonance imaging in acute ischemic stroke patients

Ronghui Huang^{1,A,D–F}, Lin Zhang^{2,B,D,F}, Limeng Deng^{1,B,C,F}, Jian-Ou Fang^{1,B,C,F}

¹ Department of Medical Imaging, The Fourth Hospital of Changsha, China

² Department of Emergency Medicine, The Fourth Hospital of Changsha, China

A – research concept and design; B – collection and/or assembly of data; C – data analysis and interpretation; D – writing the article; E – critical revision of the article; F – final approval of the article

Advances in Clinical and Experimental Medicine, ISSN 1899–5276 (print), ISSN 2451–2680 (online)

Adv Clin Exp Med. 2025;34(2):179–186

Address for correspondence

Ronghui Huang
E-mail: ronghuihuang28@163.com

Funding sources

None declared

Conflict of interest

None declared

Received on September 25, 2023

Reviewed on February 9, 2024

Accepted on February 28, 2024

Published online on April 9, 2024

Abstract

Background. Current knowledge regarding synthetic magnetic resonance imaging in ischemic stroke (MAGiC) is inadequate.

Objectives. The study aimed to investigate the diagnostic and prognostic prediction value of MAGiC in acute ischemic stroke (AIS) patients.

Materials and methods. This prospective observational study enrolled 197 AIS patients between January 2022 and May 2023. All patients underwent routine magnetic resonance imaging (MRI), computed tomography (CT) scans, doppler ultrasound, MAGiC, and dynamic contrast-enhanced (DCE)-MRI. The levels of total cholesterol (TC), triglyceride (TG), high-density lipoprotein cholesterol (HDL-ch), low-density lipoprotein cholesterol (LDL-ch), C-reactive protein (CRP), and procalcitonin (PCT) were also measured, and the National Institutes of Health Stroke Scale (NIHSS) was used to evaluate stroke severity.

Results. T2 and proton density (PD) values were markedly lower in severe patients than in mild-to-moderate patients, and the DCE-MRI K^{trans} value was substantially higher in severe patients compared to mild-to-moderate patients. Furthermore, T2 and PD correlated negatively, while K^{trans} correlated positively with CRP. Receiver operating characteristic (ROC) showed T2 and K^{trans} to have the best diagnostic potential as MAGiC and DCE-MRI parameters, respectively. As such, combining T2 and K^{trans} could improve severe stroke diagnosis accuracy. Moreover, TG, LDL-ch, CRP, T2, and K^{trans} were independent risk factors for severe stroke.

Conclusions. T2 and PD MAGiC parameters and the DCE-MRI K^{trans} parameter could be used as indices to predict severe stroke, while combining T2 and K^{trans} might provide better diagnostic accuracy.

Key words: MAGiC, ischemic stroke, DCE-MRI, diagnosis, prognosis

Cite as

Huang R, Zhang L, Deng L, Fang J. Diagnostic and prediction value of synthetic magnetic resonance imaging in acute ischemic stroke patients. *Adv Clin Exp Med.* 2025;34(2):179–186. doi:10.17219/acem/185496

DOI

10.17219/acem/185496

Copyright

Copyright by Author(s)

This is an article distributed under the terms of the Creative Commons Attribution 3.0 Unported (CC BY 3.0) (<https://creativecommons.org/licenses/by/3.0/>)

Background

Ischemic stroke accounts for more than 85% of all strokes and is the leading global cause of disability and mortality, especially in non-high-income countries.^{1,2} However, less than 5% of ischemic stroke patients receive intravenous thrombolysis.^{3,4} Generally, timely diagnosis is the critical factor for patient treatment and prognosis,⁵ and delay beyond the therapeutic time window may lead to longer treatment duration and worse prognosis.⁶

Synthetic magnetic resonance imaging (MRI), a recently developed method, can provide quantitative and qualitative T1 and T2 maps and images.⁷ A typical synthetic MRI method, magnetic resonance imaging compilation (MAGiC) from GE Healthcare (GEHC; Chicago, USA), uses multi-dynamic multi-echo (MDME).⁸ In recent years, synthetic MRI modalities such as MAGiC have been gradually applied to the diagnosis of various diseases, including Alzheimer's disease, brain cancer, multiple sclerosis, and spondyloarthritis.^{9–12} However, knowledge of MAGiC in ischemic stroke is still inadequate.

Objectives

The present study aimed to investigate the diagnostic and prognostic prediction value of MAGiC in acute ischemic stroke (AIS) patients to provide more clinical evidence and experience for MAGiC in stroke.

Materials and material

Patients

This prospective observational study enrolled 197 AIS patients admitted to our hospital between January 2022 and May 2023. The inclusion criteria were: 1) ischemic stroke diagnosed with imaging, including MRI, computed tomography (CT) and Doppler ultrasound, 2) hospital admission within 48 h of stroke, and 3) no anticoagulant treatment within 3 months of the study. The exclusion criteria were: 1) hemorrhagic stroke, 2) receiving prior anticoagulant therapy, and 3) having severe liver, cardiovascular or renal dysfunction. All patients underwent clinical tests, including imaging and laboratory evaluations on admission, and no interventions were made to the treatment. All patients provided written informed consent. Study approval was obtained from the ethical committee of the Fourth Hospital of Changsha, China (approval No. CSSDSYY-LLSC-KYXM-2019-20).

Imaging strategy

All patients received routine MRI, 3-dimensional time-of-flight (3D-TOF) magnetic resonance angiography

(MRA) for evaluation of cerebral vascular condition, CT scan, Doppler ultrasound, MAGiC, and dynamic contrast-enhanced (DCE)-MRI when admitted. All data were independently reviewed and analyzed by 2 radiologists with over 5 years of experience using the dedicated Advantage Windows AW 4.7 workstation (GE Healthcare). When discrepancies arose between the 2 radiologists, a 3rd independent radiologist was involved for re-analysis, with a consensus reached through discussion and evaluation.

For MAGiC, a SIGNA Architect 3.0T whole-body scanner (GE Healthcare) was used, and patients received routine axial (AX), T2-weighted and T1-weighted imaging with repetition time (TR) of 4,000 ms, echo time (TE) of 20/99.8 ms, echo chain length of 12, field of view (FOV) of 24 × 24, matrix of 240 × 240, section thickness of 4 mm, and bandwidth of 25.0 Hz/pixel. The data were imported into the AW 4.7 workstation to generate T1, T2 and proton density (PD) maps. The diffusion-weighted imaging (DWI) data were also imported to the AW 4.7 workstation and analyzed using the READYView package. Regions displaying a high signal on DWI and a low apparent diffusion coefficient (ADC) value were identified as infarct lesions. Subsequently, the corresponding infarct lesion on the T2 fluid-attenuated inversion recovery (T2-FLAIR) map was located, and a region of interest (ROI) was delineated to encompass the lesion. The ROI was set to 10 mm². The parameters of T1, T2 and PD within the ROI were measured twice, and the mean values were recorded.

For DCE-MRI, patients received LAVA-T1WI (flip angle = 90°, TR = 2,000 ms, TE = 45 ms, FOV = 24 × 24 cm, layer thickness = 5 mm, and layer spacing = 1 mm), LAVA-T1WI dynamic enhanced scanning with 35 phases in 1 min and 10 s (flip angle = 90°, TR = 2000 ms, TE = 45 ms, FOV = 24 × 24 cm, layer thickness = 5 mm, and layer spacing = 1 mm), following injection of gadolinium diamine (0.2 mL/kg, 3 mL/s) through the elbow vein and 15 mL normal saline (3 mL/s). The data were imported into the GenIQ package of AW 4.7 workstation, and the parameter maps of contrast agent transfer rate between blood and tissue (K^{trans}), contrast agent back-flux rate constant (K_{ep}) and extravascular extracellular fractional volume (V_e) were generated. The diffusion-weighted imaging data were also imported into the AW 4.7 workstation and analyzed using the READYView package. The infarct lesion was defined as a region exhibiting a distinctly high signal on DWI and a low ADC value. Subsequently, the DWI and aforementioned K^{trans} , K_{ep} and V_e maps were merged. The ROI was determined using the same method as before, with an area of 10 mm² to encompass the infarct lesion. The mean values of duplicate K^{trans} , K_{ep} and V_e were recorded.

Clinical characteristics

Characteristics, including age, sex, body mass index (BMI), and medical history were recorded. The levels of total cholesterol (TC), triglyceride (TG), high-density

lipoprotein cholesterol (HDL-ch), low-density lipoprotein cholesterol (LDL-ch), C-reactive protein (CRP), and procalcitonin (PCT) were evaluated on admission using an AU5800 Beckman automatic biochemical analyzer (Beckman Coulter, Brea, USA). The National Institutes of Health Stroke Scale (NIHSS) was employed to measure stroke severity as mild (<6), moderate (6–16) or severe (≥ 16).¹³

Statistical analyses

The Kolmogorov–Smirnov test assessed data normality, with non-normally distributed data expressed as median (range and interquartile range (IQR)) and normally distributed data expressed as mean \pm standard deviation (SD). Mann–Whitney U tests and t-tests compared normally or non-normally distributed data, respectively. The variance homogeneity was determined with Levene's analysis in the t-tests. Rates were compared using χ^2 tests, correlation analysis used Spearman's test, receiver operating characteristic (ROC) curves assessed diagnostic value, logistic regression was conducted using (enter method), goodness-of-fit analysis used Nagelkerke R^2 , and analysis of the linear relationship between independent variables and log-odds employed a Box–Tidwell test with Bonferroni correction. The variance inflation factor (VIF) determined multicollinearity using linear. All calculations employed IBM SPSS v. 22.0 (IBM Corp., Armonk, USA) or GraphPad Prism v. 6.0 (GraphPad Software, Inc., San Diego, USA), with $p < 0.05$ indicating a significant difference.

Results

Basic characteristics of all patients

As shown in Table 1, among all 197 ischemic stroke patients, 110 had mild-to-moderate stroke and 87 had severe stroke. The basic characteristics of the different patient groups were analyzed and compared. Levene's analysis showed TG ($p = 0.121$) and LDL-ch ($p = 0.198$) had homogeneity of variance (Supplementary Table 1). The NIHSS scores and CRP levels were significantly higher, while HDL-ch was substantially decreased in severe patients compared to the mild-to-moderate patients (all $p < 0.05$). No significant differences were found for other indices.

Comparison of MAGiC and DCE-MRI parameters for stroke patients with different severity

Typical MAGiC and DCE-MRI images are shown in Fig. 1A,B. Comparing the MAGiC and DCE-MRI parameters between mild-to-moderate and severe stroke patients showed that the T2 and PD values were remarkably lower in severe patients than in mild-to-moderate patients (both $p < 0.001$; Table 2). No significant difference was found for T1. For DCE-MRI parameters, only K^{trans} was markedly elevated in severe patients compared to the mild-to-moderate patients ($p < 0.001$), while no significant difference was found for K_{ep} or V_e .

Table 1. Basic characteristics of all patients

Variables	Mild-to-moderate patients (n = 110)	Severe patients (n = 87)	Z, t or χ^2 value*	p-value
Age [years]	61 (36–85, 27.25)	63 (35–84, 26.00)	−0.108	0.914 ^a
Sex (% female)	49 (45.79)	45 (51.72)	0.704	0.480 ^c
BMI [kg/m ²]	27.15 (19.41–33.98, 8.08)	26.66 (19.14–33.72, 7.53)	−1.077	0.281 ^a
Risk factors, n (%)	–	–	1.023	0.600 ^c
Hypertension	34 (31.78)	21 (24.14)	–	–
Diabetes	30 (28.04)	27 (31.03)	–	–
Smoking	49 (45.79)	38 (43.68)	–	–
NIHSS	8 (1–15, 8.25)	23 (16–35, 9.00)	−12.050	<0.001 ^a
TC [mmol/L]	4.41 (3.26–5.38, 1.17)	4.20 (3.25–5.33, 1.10)	−1.653	0.098 ^a
TG [mmol/L]	1.47 \pm 0.30	1.53 \pm 0.33	−1.376	0.170 ^b
HDL-ch [mmol/L]	1.09 (0.96–1.25, 0.14)	1.06 (0.95–1.24, 0.14)	−1.997	0.046 ^a
LDL-ch [mmol/L]	2.97 \pm 0.41	3.09 \pm 0.46	−1.917	0.057 ^b
CRP [mg/L]	10.20 (1.16–16.89, 7.71)	19.40 (5.64–34.66, 14.32)	−8.444	<0.001 ^a
PCT [pg/mL]	30.30 (7.79–49.89, 21.46)	28.51 (6.27–49.50, 19.97)	−0.929	0.353 ^a

*Z, t or χ^2 values were calculated with Mann–Whitney U test, t-test or χ^2 test, respectively. ^aFor non-normally distributed continuous data were expressed with median (range, interquartile range (IQR)), and p-value was calculated with Mann–Whitney U test. ^bFor non-normally distributed data expressed with (mean \pm standard deviation (SD)), p-value was calculated using t-test. ^c χ^2 test was used to analyze the rates; BMI – body mass index; NIHSS – National Institutes of Health Stroke Scale; TC – total cholesterol; TG – triglyceride; HDL-ch – high-density lipoprotein cholesterol; LDL-ch – low-density lipoprotein cholesterol; CRP – C-reactive protein; PCT – procalcitonin.

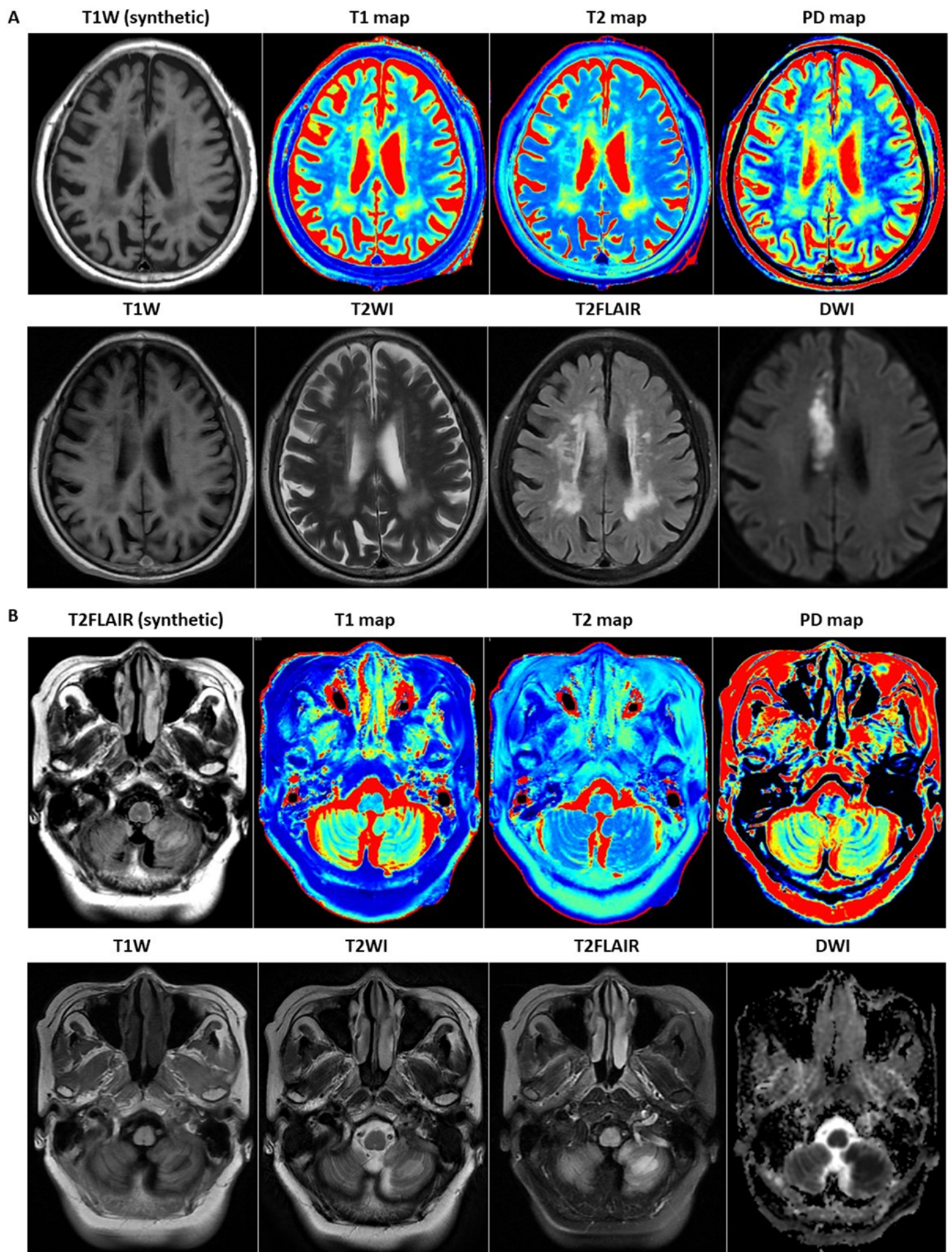


Fig. 1. A. Typical images for MAGiC and DCE-MRI of an 84-year-old female stroke patient with acute cerebral infarction in the right frontoparietal lobe. The images are synthetic T1WI, T1 map, T2 map, PD map, T1W, T2W, T2-FLAIR, and DWI; B. Typical images for MAGiC and DCE-MRI of a 63-year-old female stroke patient with multiple acute phase cerebral infarctions in the left posterior medulla oblongata and left cerebellar hemisphere. The images are listed as T2-FLAIR (synthetic), T1map, T2map, PD map, T1W, T2WI, T2-FLAIR, and DWI

MAGiC – resonance imaging in ischemic stroke; DCE-MRI – contrast-enhanced MRI; PD – proton density; DWI – diffusion-weighted imaging; FLAIR – fluid-attenuated inversion recovery.

Table 2. Comparison of MAGiC and DCE-MRI parameters for stroke patients with different severity

Variables	Mild-to-moderate patients (n = 110)	Severe patients (n = 87)	Z value*	p-value [#]
T1 [ms]	1948.95 (1503.30–2297.41, 374.68)	1894.65 (1503.26–2299.90, 488.63)	–0.435	0.663
T2 [ms]	85.46 (75.18–94.85, 11.43)	76.02 (65.47–84.94, 10.19)	–8.239	<0.001
PD [pu]	74.07 (60.28–94.75, 17.10)	68.12 (60.31–79.99, 8.14)	–4.625	<0.001
K^{trans} [min ^{–1}]	0.08 (0.05–0.12, 0.05)	0.11 (0.08–0.15, 0.04)	–7.162	<0.001
K_{ep} [min ^{–1}]	1.07 (0.10–1.90, 1.05)	1.03 (0.11–1.90, 0.92)	–0.267	–0.790
V_e [%]	7.47 (1.08–14.81, 8.01)	7.12 (1.01–14.87, 6.75)	–1.263	0.206

*Z or t values were calculated using Mann–Whitney U test. [#]All data in this table are non-normally distributed data expressed with median (range, IQR), and all p-values were calculated using Mann–Whitney U test; PD – proton density; K^{trans} – volume transfer constant; K_{ep} – rate constant; V_e – extracellular extravascular volume fraction.

Correlation between MAGiC and DCE-MRI parameters and laboratory indices

Spearman's test analyzed the correlation between MAGiC and DCE-MRI parameters and the laboratory indices, with the data shown in Supplementary Table 2. T2 and PD values were negatively correlated with CRP, while K^{trans} correlated positively. No other significant relationships were observed.

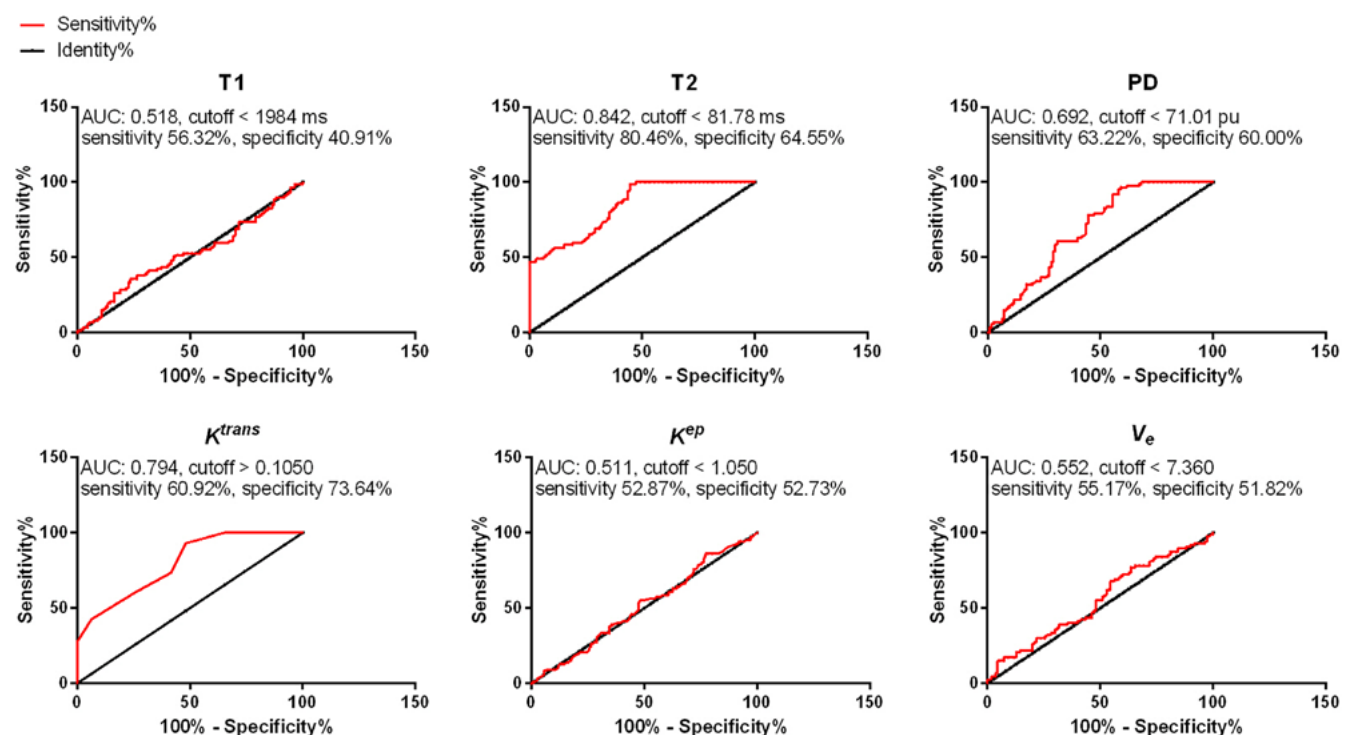
Diagnostic value of MAGiC and DCE-MRI parameters for severe stroke patients

Receiver operating characteristic curves were drawn to evaluate the diagnostic value of MAGiC and DCE-MRI parameters for severe stroke patients. As shown in Fig. 2, T2 had the best diagnostic potential in MAGiC

parameters, with an area under the curve (AUC) = 0.842, sensitivity = 80.46%, specificity = 64.55%, and a cutoff value <81.78 ms. For DCE-MRI parameters, K^{trans} showed the best diagnostic potential, with AUC = 0.794, sensitivity = 60.92%, specificity = 73.64%, and a cutoff value >0.105. We used the T2 and K^{trans} cutoff values to predict severe stroke and found that T2 had sensitivity of 64.22%, specificity of 80.68% and accuracy of 55.33%, while K^{trans} showed sensitivity of 64.63%, specificity of 70.43% and accuracy of 41.62% (Table 3). Combining both achieved sensitivity = 57.86%, specificity = 89.47% and accuracy = 71.07%.

Logistic regression for severe stroke patients

Univariate and multivariate binary logistic regression was conducted for the severe stroke risk factors. Univariate

**Fig. 2.** Receiver operating characteristic (ROC) curves of T1 (A), T2 (B), PD (C), K^{trans} (D), K_{ep} (E), and V_e (F) for diagnosis of severe stroke

PD – proton density; K^{trans} – volume transfer constant; K_{ep} – rate constant; V_e – extracellular extravascular volume fraction.

Table 3. Sensitivity, specificity and accuracy for T2 and K^{trans} to predict severe stroke

Methods	True positive	False positive	True negative	False negative	Sensitivity%	Specificity%	Accuracy%
T2	70	39	71	17	64.22	80.68	55.33
K^{trans}	53	29	81	34	64.63	70.43	41.62
T2+ K^{trans}	81	59	51	6	57.86	89.47	71.07

* Sensitivity = true positive/(true positive + false negative) × 100%; specificity = true negative/(true negative + false positive) × 100%; accuracy = (true positive + true negative)/(true positive + false negative + false positive + true negative) × 100%; K^{trans} – volume transfer constant.

Table 4. Univariate and multivariate binary logistic regression for severe stroke patients

Variables	Univariate			Multivariate		
	OR	95% CI	p-value	OR	95% CI	p-value
Age	1.002	0.983–1.022	0.805	1.004	0.975–1.033	0.808
Sex	0.757	0.430–1.330	0.333	1.024	0.434–2.415	0.956
BMI	0.965	0.904–1.029	0.277	0.980	0.885–1.085	0.697
Hypertension	0.711	0.376–1.344	0.294	1.236	0.454–3.366	0.679
Diabetes	1.200	0.647–2.227	0.563	0.646	0.248–1.683	0.371
Smoking	0.965	0.548–1.701	0.903	0.904	0.395–2.067	0.810
TC	0.696	0.446–1.086	0.110	0.710	0.374–1.351	0.297
TG	1.881	0.763–4.640	0.170	9.297	2.117–40.817	0.003
HDL-ch	0.021	0.001–0.780	0.036	0.236	0.002–36.594	0.575
LDL-ch	1.902	0.979–3.694	0.058	3.251	1.162–8.091	0.025
CRP	1.295	1.202–1.396	<0.001	0.155	0.064–0.371	<0.001
PCT	0.990	0.968–1.012	0.365	0.975	0.943–1.008	0.135
T1	1.000	0.998–1.001	0.571	0.999	0.997–1.000	0.137
T2	0.783	0.730–0.839	<0.001	11.983	4.547–31.577	<0.001
PD	0.901	0.865–0.939	<0.001	2.040	0.884–4.710	0.095
K^{trans}	2.681	1.984–3.624	<0.001	0.122	0.048–0.312	<0.001
K_{ep}	0.947	0.558–1.606	0.840	0.535	0.237–1.206	0.131
V_e	0.953	0.890–1.021	0.174	1.001	0.901–1.112	0.980

95% CI – 95% confidence interval; OR – odds ratio; BMI – body mass index; TC – total cholesterol; TG – triglyceride; HDL-ch – high-density lipoprotein cholesterol; LDL-ch – low-density lipoprotein cholesterol; CRP – C-reactive protein; PCT – procalcitonin; K^{trans} – volume transfer constant; K_{ep} – rate constant; V_e – extracellular extravascular volume fraction.

analysis found that HDL-ch, CRP, T2, PD, and K^{trans} were risk factors for severe stroke, and multivariate analysis showed that the Nagelkerke R^2 for multivariate logistic regression was 0.598. The results of the Box–Tidwell test and the VIF values are presented in Supplementary Tables 3,4. Unfortunately, the Box–Tidwell test found that CRP, T2, PD, and K^{trans} did not meet the criteria for a linear relationship. Consequently, we converted these data into categorical variables. For T2, PD and K^{trans} , we utilized the cutoff values from the previous diagnostic analysis to categorize them into low and high groups (T2 < or >81.78, PD < or >71.01 and K^{trans} < or >0.105). For CRP, we used its median value as the threshold to divide the data into low and high groups (\leq or >12.79). No variables exhibited signs of multicollinearity (VIF > 10 or tolerance <0.1). In multivariate analysis, TG, LDL-ch, CRP, T2, and K^{trans} were independent risk factors for severe stroke (Table 4).

Discussion

Despite the development of diagnostic methods, new approaches for accurate and timely diagnosis of ischemic stroke patients are always needed. In this research, we conducted a prospective observational study to investigate the application of MAGiC combined with DCE-MRI to the diagnosis of ischemic stroke patients with different severity. We found that T2, PD and K^{trans} could be used as indices to predict severe stroke, and combining T2 and K^{trans} might provide better diagnostic accuracy.

Several studies noted the potential use of MAGiC in neurological diseases, including stroke, with a recent study showing that MAGiC PSIR Vessel had a higher AUC value for vascular stenosis >50% in stroke patients than time-of-flight (TOF) magnetic resonance angiography (MRA).¹⁴ Although evidence for MAGiC in stroke patients is still inadequate, the modality is used in neurodegenerative

diseases such as Alzheimer's disease and other cognitive impairments. In Alzheimer's disease, MAGiC T1 and T2 values in the right insula cortex and left hippocampus were markedly increased compared to controls.¹⁵ Another study used synthetic MRI to detect white matter hyperintensities (WMHs) and found a significant association between myelin loss and WMHs in cognitively impaired patients.¹⁶ Additionally, a recent study demonstrated that patients with primary insomnia showed a negative correlation between cerebral blood flow and MAGiC T2 values.¹⁷

The current study showed that T2 and PD values were lower in severe stroke patients, with AUC of 0.842 and 0.692, respectively, and could be used as a diagnostic marker. In addition, we found that T2 and PD values correlated negatively with CRP levels and identified T2 and CRP values as independent risk factors for severe stroke. Given that severe stroke is often associated with an activated inflammatory response, we hypothesize a potential connection between T2 values and inflammatory conditions. However, it is premature to draw definitive conclusions without further investigation.

DCE-MRI is widely used in stroke diagnosis, with early studies showing that it could measure atherosclerotic plaques, blood–brain barrier function, and vascular and hemodynamic features.^{18–20} A recent study reported convolutional neural networks, which provided better DCE-MRI efficacy in stroke diagnosis.²¹ In an animal model of stroke, DCE-MRI measured post-stroke outcome, angiogenesis and vascular function.²² In our investigation, we observed that K^{trans} was markedly increased in severe stroke patients and that combining T2 and K^{trans} showed better diagnostic accuracy for severe stroke. Furthermore, K^{trans} correlated positively with CRP levels. Similar to the T2 value, we speculate that K^{trans} might partially reflect the inflammatory condition in stroke patients. However, this hypothesis requires more comprehensive studies to gain deeper insights.

Limitations

Study limitations include 1) enrolling 197 patients who were from a single center and 2) the focus on short-term clinical outcomes of the ischemic stroke patients. As such, whether MAGiC could provide indications for patients' long-term condition is unclear.

Conclusions

Magnetic resonance imaging in ischemic stroke can be used to predict ischemic stroke severity, with T2 and PD showing potential as prediction markers. The combination of T2 and K^{trans} may provide a new assessment method for the diagnosis of severe stroke patients. This study may provide more clinical evidence for the application of MAGiC in the diagnosis of ischemic stroke.

Supplementary data

The Supplementary materials are available at <https://doi.org/10.5281/zenodo.10838478>. The package includes the following files:

Supplementary Table 1. Original results of t-test and Levene analysis for TG and LDL-ch in t-test of Table 1.

Supplementary Table 2. Spearman's correlation among MAGiC and DCE-MRI parameters and the laboratory indices.

Supplementary Table 3. Box–Tidwell test for all variables in logistic regression analysis.

Supplementary Table 4. Box–Tidwell test for all variables in logistic regression analysis.

Data availability


The datasets generated and/or analyzed during the current study are available from the corresponding author on reasonable request.

Consent for publication


Not applicable.

ORCID iDs

Ronghui Huang  <https://orcid.org/0009-0007-9211-6009>

Lin Zhang  <https://orcid.org/0009-0001-5009-7432>

Limeng Deng  <https://orcid.org/0009-0001-4111-1685>

Jian-Ou Fang  <https://orcid.org/0009-0008-2204-8968>

References

- Barthels D, Das H. Current advances in ischemic stroke research and therapies. *Biochim Biophys Acta Mol Basis Dis*. 2020;1866(4):165260. doi:10.1016/j.bbdis.2018.09.012
- Feigin VL, Brainin M, Norrving B, et al. World Stroke Organization (WSO): Global Stroke Fact Sheet 2022. *Int J Stroke*. 2022;17(1):18–29. doi:10.1177/17474930211065917
- Saini V, Guada L, Yavagal DR. Global epidemiology of stroke and access to acute ischemic stroke interventions. *Neurology*. 2021;97(20 Suppl 2). doi:10.1212/WNL.00000000000012781
- Pohl M, Hessezenberger D, Kapus K, et al. Ischemic stroke mimics: A comprehensive review. *J Clin Neurosci*. 2021;93:174–182. doi:10.1016/j.jocn.2021.09.025
- Kuriakose D, Xiao Z. Pathophysiology and treatment of stroke: Present status and future perspectives. *Int J Mol Sci*. 2020;21(20):7609. doi:10.3390/ijms21207609
- Rabinstein AA. Update on treatment of acute ischemic stroke. *Continuum (Minneapolis)*. 2020;26(2):268–286. doi:10.1212/CON.0000000000000840
- Lee C, Choi YJ, Jeon KJ, Han SS. Synthetic magnetic resonance imaging for quantitative parameter evaluation of temporomandibular joint disorders. *Dentomaxillofac Radiol*. 2021;50(5):20200584. doi:10.1259/dmfr.20200584
- Konar AS, Paudyal R, Shah AD, et al. Qualitative and Quantitative Performance of Magnetic Resonance Image Compilation (MAGiC) method: An exploratory analysis for head and neck imaging. *Cancers (Basel)*. 2022;14(15):3624. doi:10.3390/cancers14153624
- Konar AS, Shah AD, Paudyal R, et al. Quantitative synthetic magnetic resonance imaging for brain metastases: A feasibility study. *Cancers (Basel)*. 2022;14(11):2651. doi:10.3390/cancers14112651
- Krauss W, Gunnarsson M, Nilsson M, Thunberg P. Conventional and synthetic MRI in multiple sclerosis: A comparative study. *Eur Radiol*. 2018;28(4):1692–1700. doi:10.1007/s00330-017-5100-9

11. Zhang K, Liu C, Zhu Y, et al. Synthetic MRI in the detection and quantitative evaluation of sacroiliac joint lesions in axial spondyloarthritis. *Front Immunol.* 2022;13:1000314. doi:10.3389/fimmu.2022.1000314
12. Lin W, Lin W, Chen G, et al. Bidirectional mapping of brain MRI and PET with 3D reversible GAN for the diagnosis of Alzheimer's disease. *Front Neurosci.* 2021;15:646013. doi:10.3389/fnins.2021.646013
13. Fang YN, Tong MS, Sung PH, et al. Higher neutrophil counts and neutrophil-to-lymphocyte ratio predict prognostic outcomes in patients after non-atrial fibrillation-caused ischemic stroke. *Biomed J.* 2017;40(3):154–162. doi:10.1016/j.bj.2017.03.002
14. Wang Q, Wang G, Sun Q, Sun DH. Application of MAGnetic resonance imaging compilation in acute ischemic stroke. *World J Clin Cases.* 2021;9(35):10828–10837. doi:10.12998/wjcc.v9.i35.10828
15. Lou B, Jiang Y, Li C, et al. Quantitative analysis of synthetic magnetic resonance imaging in Alzheimer's disease. *Front Aging Neurosci.* 2021;13:638731. doi:10.3389/fnagi.2021.638731
16. Park M, Moon Y, Han SH, Kim HK, Moon WJ. Myelin loss in white matter hyperintensities and normal-appearing white matter of cognitively impaired patients: A quantitative synthetic magnetic resonance imaging study. *Eur Radiol.* 2019;29(9):4914–4921. doi:10.1007/s00330-018-5836-x
17. Luo XW, Li QX, Shen LS, et al. Quantitative association of cerebral blood flow, relaxation times and proton density in young and middle-aged primary insomnia patients: A prospective study using three-dimensional arterial spin labeling and synthetic magnetic resonance imaging. *Front Neurosci.* 2023;17:1099911. doi:10.3389/fnins.2023.1099911
18. Van Hoof RHM, Heeneman S, Wildberger JE, Kooi ME. Dynamic contrast-enhanced MRI to study atherosclerotic plaque microvasculature. *Curr Atheroscler Rep.* 2016;18(6):33. doi:10.1007/s11883-016-0583-4
19. Villringer K, Sanz Cuesta BE, Ostwaldt AC, et al. DCE-MRI blood–brain barrier assessment in acute ischemic stroke. *Neurology.* 2017;88(5):433–440. doi:10.1212/WNL.0000000000003566
20. Quarles CC, Bell LC, Stokes AM. Imaging vascular and hemodynamic features of the brain using dynamic susceptibility contrast and dynamic contrast enhanced MRI. *NeuroImage.* 2019;187:32–55. doi:10.1016/j.neuroimage.2018.04.069
21. Ulas C, Das D, Thrippleton MJ, et al. Convolutional neural networks for direct inference of pharmacokinetic parameters: Application to stroke dynamic contrast-enhanced MRI. *Front Neurol.* 2019;9:1147. doi:10.3389/fneur.2018.01147
22. Pradillo JM, Hernández-Jiménez M, Fernández-Valle ME, et al. Influence of metabolic syndrome on post-stroke outcome, angiogenesis and vascular function in old rats determined by dynamic contrast enhanced MRI. *J Cereb Blood Flow Metab.* 2021;41(7):1692–1706. doi:10.1177/0271678X20976412